Chapter 45
Cortical Anatomy and the Spatiotemporal Learning Rule

J.J. Wright and P.D. Bourke

Abstract A model of the self-organization of synapses in the visual cortex is presented. Subject to Hebbian learning with decay, evolution of synaptic strengths proceeds to a stable state in which all synapses have either maximum, or minimum, pre/post-synaptic coincidence. The most stable configuration gives rise to anatomically realistic "local maps", each of macro-columnar size, and each organized as Mobius projections of retinotopic space. A tiling of V1, constructed of approximately mirror-image reflections of each local map by its neighbors is formed, accounting for orientation-preference singularities, linear zones, and saddle points—with each map linked by connections between sites of common orientation preference. Ocular dominance columns, the occurrence of direction preference fractures always in odd numbers around singularities, and effects of stimulus orientation relative to velocity of motion, are accounted for. Convergence to this configuration is facilitated by the spatio-temporal learning rule.

Keywords

AQ1

Introduction

We have presented a theoretical account of the self-organization of synapses during development of the visual cortex (V1) [1]. This theory deduced the most stable configuration of synapses to emerge under a Hebbian learning rule. No consideration was given to pre-synaptic interaction, nor was a specific physiology of synaptic modification invoked. The spatiotemporal learning rule [2, 3] – which was developed in relation to work in the hippocampus – allows for pre-synaptic interactions, and relates pre- and post-synaptic interactions to long-term-potentiation (LTP) and depression (LTD). This paper summarizes the earlier theory of V1 self-organization, and concludes with comments on the relevance of the spatiotemporal rule in this further anatomical context.

J.J. Wright
Department of Psychological Medicine, University of Auckland, Auckland, New Zealand
e-mail: jj.w@xtra.co.nz

R. Wang et al. (eds.), *Advances in Cognitive Neurodynamics ICCN 2007*,

Theory

Synaptic Densities in V1

In V1 and cortex generally, the density of synaptic couplings generated by each neuron declines with distance from the soma of the cell of origin, at two principal scales – that of the local intra-cortical connections (at the V1 macrocolumnar scale), versus the longer intracortical connections spanning a substantial fraction of the extent of the V1, which are continuous with interareal connections [4, 5, 6]. Via polysynaptic transmission, information can reach each macrocolumn-sized area, from the whole, or a substantial part, of V1, thus modulating direct visual pathway inputs. We will describe the emergent unit organization on the smaller, macrocolumnar, scale as the *local map*, and V1 itself as the *global map*.

Visual Cross-Correlation and Synchronous Fields

Because of the decline of synaptic density with distance, the spatial covariance of activity (synchronous oscillation) between any pair of pyramidal neurons in V1 declines with distance [7, 8, 9, 10]. Visual stimuli exhibit a decline in spatial covariance with distance, and impose this property upon activity in V1. Thus, covariance of activity in V1 declines with distance at both the global, V1, scale, and the local, macro-columnar, scale, and as will be shown, this provides a metric for organization of connections.

Learning Rule

A simple Hebbian rule, with decay can be initially applied. At each synapse the co-incidence of pre and post synaptic activity, $r_{Q\varphi}$, over a short epoch, t, is given by

$$r_{Q\varphi}(t) \propto \sum\nolimits_t Q_e(t) \times \varphi_e(t) \tag{45.1}$$

where $Q_e(t) \in \{0, 1\}$ is the post-synaptic firing rate, and $\varphi_e(t) \in \{0, 1\}$ is the pre-synaptic firing rate. A Hebbian multiplication factor, H_s, operating on the gain of synapses at steady states of pre- and post-synaptic firing is given as

$$H_s = H_{\max} \exp\left[-\lambda / r_{Q\varphi} \right] \tag{45.2}$$

where λ is a suitable constant. With changes in $r_{Q\varphi}$, H_s can increase or decline over time.

Stability at Individual Synapses

It is shown in [1] that under this learning rule synapses can approach a stable state, only by approaching either one of two extremes – either *saturated* or *sensitive*.

In the saturated state, H_s and $r_{Q\varphi}$ are at maxima, while in the sensitive state, H_s and $r_{Q\varphi}$ are at minima. Conversely, $\frac{dH_s}{dr_{Q\varphi}}$, the sensitivity to change in synaptic gain, is at a minimum for saturated synapses and a maximum for sensitive synapses – hence the choice of the names. No specific physiological state was assumed as the basis of saturation or sensitivity.

Metabolic Uniformity

Competition occurring for metabolic resources within axons adds a constraint to Hebbian rules [11]. Metabolic energy supply of all small axonal segments remains approximately uniform, while the metabolic demand of saturated synapses, which have high activity, will be much greater than for sensitive synapses. Therefore the proportion of saturated and sensitive synapses must be approximately uniform along axons, and consequently the densities of both saturated and sensitive synapses must decline with distance of pre-synapses from the cell bodies of origin.

The Impact of Distance/Density and Saturation/Sensitivity on Overall Synaptic Stability

All positions in V1, $\{P_{j,k}\}$, can be given an ordered numbering in the complex plane, $1 \ldots, j, \ldots, k, \ldots, 2n$, and all positions within a macrocolumn located at P_0, $\{P_{j,k}\}$, can be similarly numbered. The total perturbation of synaptic gains for the synapses from V1 entering the macrocolumn, $\Psi(pP)$, and the total perturbation of synaptic gains within the macrocolumn, $\Psi(pp)$, can thus be written as

$$\Psi(pP) = \sum_{j=1}^{j=n}\sum_{k=1}^{k=n} \sigma_{SAT}(p_jP_k)S_{SAT}(p_jP_k) + \sum_{j=1}^{j=n}\sum_{k=1}^{k=n} \sigma_{SENS}(p_jP_k)S_{SENS}(p_jP_k) \tag{45.3}$$

$$\Psi(pp) = \sum_{j=1}^{j=n}\sum_{k=1}^{k=n} \sigma_{SAT}(p_jp_k)S_{SAT}(p_jp_k) + \sum_{j=1}^{j=n}\sum_{k=1}^{k=n} \sigma_{SENS}(p_jp_k)S_{SENS}(p_jp_k) \tag{45.4}$$

where $\sigma_{SAT}(p_jP_k, p_jp_k)$ and $\sigma_{SENS}(p_jP_k, p_jp_k)$ are densities of saturated and sensitive synapses respectively, and $S_{SAT}(p_jP_k, p_jp_k)$ and $S_{SENS}(p_jP_k, p_jp_k)$ are the corresponding variations of synaptic gains over a convenient short epoch.

Since densities of synapses decline with distances of cell separation, then as a simple arithmetic property of sums of products, minimization of $\Psi(pp)$ requires neurons separated by short distances to most closely approach maximum saturation, or maximum sensitivity. Yet metabolic uniformity requires that both sensitive and saturated synaptic densities must decline with distance from the cell bodies of origin, and remain in equal ratio. An apparent paradox arises, since sensitive synapses must link pre- and post-synaptic neurons with minimal pre- and post-synaptic pulse co-incidence, yet the reverse is true for saturated synapses. Also apparently paradoxically, minimization of $\Psi(pP)$ requires that saturated connections afferent to any p_j arise from highly covariant, and therefore closely situated, sites in V1, while sensitive connections afferent to p_j must arise from well-separated sites. Yet again, metabolic uniformity requires that both sensitive and saturated pre-synapses arise from cells at any single site. The paradoxes exist only in the Euclidean plane, and can be resolved as follows.

Mobius Projection, and the Local Map

By re-numbering $\{P_{j,k}\}$ as $\{P_{j1,j2,k1,k2}\}$, and $\{p_{j,k}\}$ as $\{p_{j1,j2,k1,k2}\}$, the subscript numbers $1, \ldots, j1, \ldots, j2, \ldots, n, (n+1), \ldots, j2, \ldots, k2, \ldots, 2n$ can be ascribed in the global map so that $j1$ and $j2$ are located diametrically opposite and equidistant from P_0, while in the local map $j1$ and $j2$ have positions analogous to superimposed points located on opposite surfaces of a Mobius strip. This generates a *Mobius projection* (the *input map*) from global to local, and a *Mobius ordering* within the local map. That is,

$$\frac{P_{jm}^2}{|P_{jm}|} \rightarrow p_{km} \quad m \in \{1, 2\} \tag{45.5}$$

$$p_{jm} \rightarrow p_{km} \qquad m \in \{1, 2\} \tag{45.6}$$

In Eq. (45.5) the mapping of widely separated points in the global map converge to coincident points on opposite surfaces of the local map's Mobius representation. In the Eq. (45.6) the density of saturated synaptic connections now decreases as $|j1-k1|$ and $|j2-k2|$, while the density of sensitive couplings decreases as $|j2-k1|$ and $|j1-k2|$.

The anatomical parallel requires $j1$ and $j2$ in the local map to represent two distinct groups of neurons. To attain maximum synaptic stability within the local map an intertwined mesh of saturated couplings forms, closed after passing twice around the local map's centre, with sensitive synapses locally linking the two turns of the mesh together. In this fashion both saturated and sensitive synapses decline in density with distance, as required. The input map is of corresponding form, conveying an image of the activity in V1 analogous to projection onto a Mobius strip.

Evolution of these patterns of synaptic connections is shown in Figs. 45.1 and 45.2.

Fig. 45.1 Initial conditions for local evolution of synaptic strength. *Left*: The global field (V1) in polar co-ordinates. Central defect indicates the position of a local area of macro-columnar size. Polar angle is shown by the color spectrum, twice repeated. *Middle:* Zones of random termination (shown by color) of lateral axonal projections from global V1 in the local area. Central defect is an arbitrary zero reference. *Right*: Transient patterns of synchronous oscillation generated in the local area, mediated by local axonal connections

Fig. 45.2 Evolution of synaptic strengths to their maximally stable configuration. *Left*: The global field (V1), as represented in Fig. 45.1. *Middle*: Saturated synaptic connections input from the global field now form a Mobius projection of the global field, afferent to the local map, forming an input map. *Right*: Saturated local synapses within the local map form a mesh of connections closed over 0–4π radians. The central defect now corresponds to the position within the local map, of the local map within the global map. Sensitive synapses (not shown) link adjacent neurons as bridges between the 0–2π and 2π–4π limbs of the mesh of saturated connections. Wright et al. 2006

Monosynaptic Interactions Between Adjacent Local Maps

The input and local maps can, in principle, emerge with any orientation, and with either left or right-handed chirality. However, chirality and orientation of adjacent local maps is also constrained by requirement for overall stability. Adjacent local maps should form in approximately mirror image relation, as shown in Fig. 45.3, because in that configuration homologous points within the local maps have densest saturated and sensitive synaptic connections, thus meeting minimization requirements analogous to those of Eq. 45.3a,b.

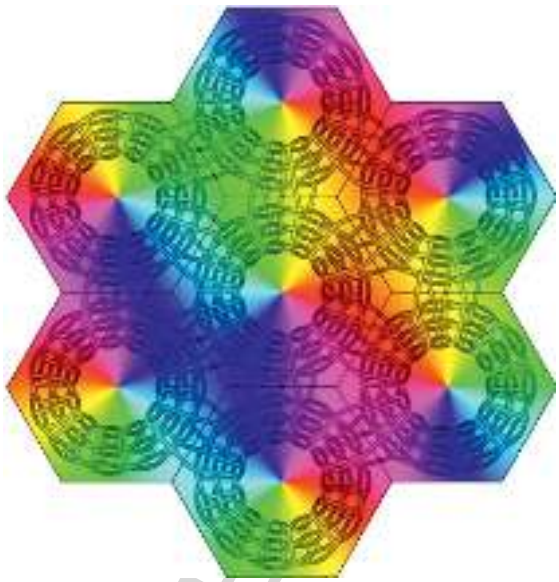

Fig. 45.3 Organization of saturated coupling within and between local maps, and the approximate mirror symmetry of orientation preference in adjacent local maps [1]

Consequences of Projection of Object Configuration and Motion from the Global to the Local Map

The emergent input and local maps form a 1:1 representation of points in the global map. As described in [1], this accounts for response preferences of V1 neurons to visual stimuli – notably orientation preference singularities, linear zones and saddle points, and connections between cells of similar orientation preference in adjacent macrocolumns [12]. Ocular dominance columns [13], which arise in parts of V1 with binocular input, can be explained as a special case of the application of similar mechanisms to those operating in monocular cortex. The occurrence of direction preference fractures always in odd numbers around singularities [14] is explained by the Mobius configuration of the local map, and axonal conduction lags from the global to the local maps accounts for the dynamic variation of orientation preference which occurs with changes in stimulus velocity when, stimulus orientation is not orthogonal to the direction of motion [15].

Application of the Spatiotemporal learning Rule and its Relationship to LTP and LTD

The explanation of self-organization of the synaptic connections in V1 given in[1] is deficient in two respects.

Firstly, no particular physiological synaptic mechanism is associated with the descriptive terms “saturated” and “sensitive”, and these idealized states may never be attained physiologically. However, at least on the appropriate time-scale, saturation

of a synapse may be equated with the LTP state, and sensitivity of a synapse with the LTD state, as indicated in [2, 3].

Secondly, the approach of all synapses to their maximally stable condition has been assumed, without any mechanism being proposed to assist convergence towards maximum stability. The spatiotemporal rule has been recently specified in relation to LTD/LTP of conventional Hebbian type [16]. The operation of this learning rule, which facilitates the mapping of adjacent afferent connections, has the properties required to bring about convergence to stability, since the global-to-local mapping depends on the preservation of the same relation between spatial covariance and distance at both local and global levels.

References

1. Wright JJ, Alexander DM, Bourke PD (2006) Contribution of lateral interactions in V1 to organization of response properties. Vision Research 46: 2703–2720.
2. Tsukada M, Aihara T, Saito H (1996) Hippocampal LTP depends on spatial and temporal correlation of inputs. Neural Networks 9: 1357–1365.
3. Tsukada M, Pan X (2005) The spatio-temporal learning rule and its efficiency in separating spatiotemporal patterns. Biological Cybernetics 92: 139–146.
4. Scholl DA (1956) The Organization of the Cerebral Cortex. Wiley, New York.
5. Braitenberg V, Schuz A (1991) Anatomy of the Cortex: Statistics and Geometry. Springer-Verlag, New York.
6. Liley DTJ, Wright JJ (1994) Intracortical connectivity of pyramidal and stellate cells: estimates of synaptic densities and coupling symmetry. Network 5: 175–189.
7. Wright JJ (1997) EEG simulation: variation of spectral envelope, pulse synchrony and 40 Hz oscillation. Biological Cybernetics 76: 181–184.
8. Robinson PA, Rennie CJ, Wright JJ (1998) Synchronous oscillations in the cerebral cortex. Physical Review E 57: 4578–4588.
9. Wright JJ, Bourke PD, Chapman CL (2000) Synchronous oscillation in the cerebral cortex and object coherence: simulation of basic electrophysiological findings. Biological Cybernetics 83: 341–353.
10. Chapman CL, Bourke PD, Wright JJ (2002) Spatial eigenmodes and synchronous oscillation: coincidence detection in simulated cerebral cortex. Journal of Mathematical Biology 45: 57–78.
11. Grossberg S, Williamson JR (2001) A neural model of how horizontal and interlaminar connections of visual cortex develop into adult circuits that carry out perceptual grouping and learning. Cerebral Cortex 11: 37–58.
12. Bosking WH, Zhang Y, Schofield B, Fitzpatrick D (1997) Orientation selectivity and the arrangement of horizontal connections in tree shrew striate cortex. Journal of Neuroscience 17: 2112–2127.
13. Obermayer K, Blasdel GG (1993) Geometry of orientation and ocular dominance columns in monkey striate cortex. Journal of Neuroscience 13: 4114–4129.
14. Swindale NV, Shoham D, Grinvald A, Bonhoeffer T, Hubener M. (2000) Visual cortical maps are optimised for uniform coverage. Nature Neuroscience 3: 822–826.
15. Basole A, White LE, Fitzpatrick D (2003) Mapping multiple features of the population response of visual cortex. Nature 423: 986–990.
16. Tsukada M, Yamazaki Y, Kojima H (2007) Interaction between the spatiotemporal learning rule (STRL) and Hebb type (HEBB) in single pyramidal cells in the hippocampal CA1 area. (in submission).

AQ2